

Purification, Reconstitution, and Subunit Composition of a Voltage-Gated Chloride Channel from *Torpedo* Electropex[†]

Richard E. Middleton, Deborah J. Pheasant, and Christopher Miller*

Howard Hughes Medical Institute, Graduate Department of Biochemistry, Brandeis University, Waltham, Massachusetts 02254

Received July 5, 1994; Revised Manuscript Received August 29, 1994[®]

ABSTRACT: The voltage-gated Cl[−] channel from *Torpedo* electropex was purified in functional form by an immunoaffinity procedure. Channel activity was assayed by ³⁶Cl[−] uptake into reconstituted liposomes and by direct recording after insertion into planar lipid bilayers. The purified channel displays the same “double-barreled” gating kinetics observed with native membranes, as well as the correct single-channel permeation characteristics. Preparations of active channels consist of a 90-kDa polypeptide, as expected from the known cDNA sequence. No associated subunits are present in the purified material. Direct protein sequencing confirms the absence of a cleavable signal sequence and demonstrates an N-terminus at Ser-2 of the cDNA-derived sequence. This “ClC-0” protein is lightly glycosylated, losing only ≈2 kDa of sugar upon treatment with endoglycosidase H or N-glycanase. Most if not all of this glycosylation is found on Asn-365. This result necessitates revision of current transmembrane topology proposals, which have placed this residue on the cytoplasmic side of the membrane. Sedimentation in sucrose density gradients under activity-preserving conditions suggests the ClC-0 channel is slightly larger than the Na/K-ATPase α/β-protomer (≈150 kDa) and substantially smaller than the reduced form of the nicotinic acetylcholine receptor (≈300 kDa). The detergent-solubilized ClC-0 channel, which invariably displays two Cl[−] diffusion pores in the active complex, is therefore built most likely as a homodimer of the 90-kDa protein purified here.

Chloride-selective channels are found in the plasma membranes of nearly all vertebrate cells (Franciolini & Petris, 1990). These channels operate in diverse physiological contexts, such as cell volume regulation, transepithelial electrolyte transport, and tuning of neuronal electrical activity. One of the best-understood examples is found in mammalian skeletal muscle, where voltage-gated Cl[−] channels dominate the resting membrane conductance and set the highly negative resting potential of this tissue; dysfunction of muscle Cl[−] channels underlies the membrane hyperexcitability originally recognized in certain animal myotonias (Bryant, 1973; Palade & Barchi, 1977), and is now known to cause certain inherited myotonias in humans as well (Koch et al., 1992).

At the molecular level, no unifying picture of the Cl[−] channels has yet emerged, as exists, for example, for the voltage-gated cation channels (Sigworth, 1994). Though numerous genes encoding Cl[−] channels have been identified, and several Cl[−] channels have been purified from epithelial tissues (Ran & Benos, 1992; Redhead et al., 1992; Finn et al., 1993), most of these share no molecular characteristics with the others. In only a single case has a homologous set of Cl[−] channels been found, the “ClC family”. The founding member of this family, ClC-0, was cloned from the electric organ of the marine ray *Torpedo* (Jentsch et al., 1990), and homologous channels are specifically found in mammalian muscle (Steinmeyer et al., 1991), kidney (Uchida et al., 1993), and brain (Kawasaki et al., 1994). A closely related channel is expressed ubiquitously and is activated by hypotonicity (Gründer et al., 1992). These ClC-type chan-

nels all encode proteins of 75–110 kilodaltons (kDa)¹ and contain 12 or 13 hydrophobic stretches long enough to form transmembrane α-helices.

Heterologous expression studies strongly argue that functional channels require expression of only the ClC-type cDNAs (Bauer et al., 1991), but the subunit composition of the assembled channels in natural tissues is entirely unknown. We have no information, for instance, on the existence of “helper” subunits, which in Na⁺, K⁺, and Ca²⁺ channels boost expression levels or modify gating kinetics (Parcej & Dolly, 1989; Rettig et al., 1994; Knaus et al., 1994; Isom et al., 1994). Nor is the number of ClC subunits required to build a functional channel known. Likewise, the molecular architecture and transmembrane topology of ClC channels are only weakly suggested from sequence analysis. These holes in our molecular view of ClC channels result from the absence of direct information about these channels at the protein–biochemical level. This provides the motivation for the work described here: the purification and functional reconstitution of ClC-0, the voltage-gated Cl[−] channel of *Torpedo* electric organ.

¹ Abbreviations: BCA protein assay, bicinchoninic acid protein assay from Pierce (no. 23235); BCIP, 5-bromo-4-chloro-3-indolyl 1-phosphate; CHAPS, 3-[(3-cholamidopropyl)dimethylammonio]-1-propanesulfonate; DEAE, diethylaminoethyl; DTT, dithiothreitol; EGTA, ethylene glycol bis(β-aminoethyl ether)-N,N,N',N'-tetraacetic acid; HEPES, N-(2-hydroxyethyl)piperazine-N'-2-ethanesulfonic acid; kDa, kilodalton(s); lipid mix, 5:1:2:2 molar ratio of L-α-phosphatidylethanolamine/L-α-phosphatidylcholine/L-α-phosphatidylserine/cholesterol; NBT, nitro blue tetrazolium; PAGE, polyacrylamide gel electrophoresis; PBS, 125 mM NaCl/25 mM sodium phosphate, pH 7.2; SDS, sodium dodecyl sulfate; SITS, 4-acetamido-4'-isothiocyano stilbene-2,2'-disulfonic acid; TCA, trichloroacetic acid; Tris, tris(hydroxymethyl)aminomethane.

[†] This research was supported in part by NIH Grant GM-31768.

[®] Abstract published in *Advance ACS Abstracts*, October 15, 1994.

We choose CIC-0 as our target for two reasons. First, this is the only CIC-type channel whose functional properties have been described in detail at both macroscopic and single-channel levels [for a review, see Miller and Richard (1990)]. In broad analogy to voltage-gated cation channels, CIC-0 displays two main gating processes, fast "activation" and slower "inactivation", both of which are favored by membrane depolarization. In contrast to voltage-gated cation channels, in CIC-0 the voltage ranges of these two processes are well separated, so that there is a wide window of voltage over which open channels can be observed at equilibrium. The most striking characteristic of CIC-0 is its "binomial" single-channel behavior. Channel openings always appear in bursts of activity revealing three conductance levels of 0, 10, and 20 pS in 150 mM Cl^- . This behavior has been proposed (Miller, 1982) to reflect a "double-barreled" conducting unit composed of two identical protochannels, each of which exhibits fast activation gating. According to this structural model, which is supported by numerous lines of indirect evidence (Miller & Richard, 1990), these two identical Cl^- conduction pathways are gated simultaneously by the slow inactivation process. This double-barreled gating is preserved in the channel formed by heterologous expression of CIC-0 alone in *Xenopus* oocytes (Bauer et al., 1991).

The second rationale for choosing CIC-0 for a biochemical attack is its abundance in the *Torpedo* electrocyte. Goldberg and Miller (1991) applied a reconstitution assay based on $^{36}\text{Cl}^-$ fluxes in liposomes to develop conditions for solubilizing CIC-0 in detergent micelles and maintaining its activity. While conventional chromatographic methods did not achieve purification of the channel, these studies were able to estimate the absolute density of CIC-0 in the electric organ, 2–4% of the membrane protein. The *Torpedo* electric organ thus provides an extremely rich source for future structural analysis of a Cl^- channel, just as the same tissue has permitted the only high-resolution structure of a eukaryotic ion channel, the nicotinic acetylcholine receptor (Unwin, 1993).

We now report the analytical-scale purification of fully functional CIC-0 channels from *Torpedo californica* electric organ. The one-step procedure utilizes an immunoaffinity strategy based on purified polyclonal antibodies raised to a peptide taken from the sequence of CIC-0. The purified channel behaves quantitatively as expected when assayed either by Cl^- fluxes in liposomes or by direct electrical recording after insertion of single channels into planar lipid bilayer membranes. Only a single glycoprotein band, which corresponds to the CIC-0 sequence, is observed in the purified channel, and the active complex sediments in sucrose density gradients as a homodimer of this 90-kDa protein.

MATERIALS AND METHODS

Materials. *Torpedo californica* electrocyte membranes enriched in Cl^- channels were prepared as described previously (Goldberg & Miller, 1991) with recent modifications (Middleton et al., 1994). [^{36}Cl]Chloride (≈ 10 mCi/g) was purchased from New England Nuclear. L- α -Phosphatidylcholine (PC), L- α -phosphatidylethanolamine (PE), and L- α -phosphatidylserine (PS) from bovine brain were purchased from Avanti Polar Lipids as 10 mg/mL solutions in chloroform and were stored in sealed ampules at -70°C . Ergosterol and cholesterol were from Sigma and were

recrystallized from 100% ethanol before use. A mixture of PC, PE, PS, and cholesterol (or ergosterol) was prepared in a 5:1:2:2 molar ratio ("lipid mix") and stored under nitrogen at -70°C . Sephadex G-50 (fine) was from Pharmacia. 3-[(3-Cholamidopropyl)dimethylammonio]-1-propanesulfonate (CHAPS) was from Pierce. Dowex 1 (Cl^- form, $1 \times 4-100$), nystatin, endoglycosidase H, and Freund's adjuvant were from Sigma. Recombinant N-glycanase was from Genzyme. NP-40 and Triton X-114 were from Calbiochem. Triton X-100 and Triton X-405 were from Aldrich. Mercaptoethanol was from Bio-Rad. Alkaline phosphatase-conjugated anti-rabbit IgG, NBT, and BCIP were from Promega. V8 protease was from ICN Biomedicals.

Generation and Purification of Anti-CIC-0 Antibodies. Anti-CIC-0 antibodies were raised in New Zealand white rabbits (female) by subcutaneous injections of a fusion protein (200–500 μg in Freund's adjuvant) that contained 18 amino acids of CIC-0 beginning at Glu-642 (EGQQREGLEAVKVQTEDP; Jentsch et al., 1990). The phage T7 gene-9 fusion protein was overexpressed in *Escherichia coli* BL21(DE3) and partially purified as described previously (Park et al., 1991). The plasmid used to express the gene-9 fusion protein was constructed from pCSP105 by ligation of synthetic oligonucleotides coding for the CIC-0 sequence into the *SalI* and *HindIII* restriction sites. The fusion protein was partially purified on a DEAE column, and then further purified by SDS-PAGE on a preparative 10% slab gel. The fusion protein was excised from the gel and passively eluted overnight into 0.25% SDS/1.0 mM DTT/0.1 M NH_4HCO_3 , pH 8.4. The fusion protein was concentrated, acetone-precipitated, and resuspended in 10 mM Tris, pH 6.8.

The anti-CIC-0 specific antibodies were purified from rabbit serum on a peptide affinity column. A synthetic peptide containing the same residues from CIC-0 that were included in the fusion protein was immobilized on a Pierce SulfoLink gel (1 mL) via an amino-terminal cysteine. Serum was diluted 5-fold into PBS (125 mM NaCl/25 mM Na_2HPO_4 , pH 7.2) and allowed to flow through the peptide affinity column. The column was washed with 10 mL of PBS, 5 mL of PBS containing an additional 150 mM NaCl, and then with PBS until the absorbance at 280 nm was below 0.04. The antibodies were eluted with 1 mL aliquots of 0.1 M glycine, pH 2.5, and the absorbance at 280 nm was monitored.

SDS-PAGE and Western Blots. Proteins were separated by electrophoresis on either 7.5% or 12% acrylamide SDS-PAGE gels (Laemmli, 1970) using the BioRad Mini-PROTEAN II apparatus. Polypeptides were visualized by Coomassie blue or silver-stain. The procedure of Merrill et al. (1981) was used for silver-staining except that gels were soaked in 0.8 mM sodium thiosulfate/0.02% formalin for 60 s instead of potassium dichromate/nitric acid.

Anti-CIC-0 serum and CIC-0-specific antibodies were assayed by Western blots. After SDS-PAGE, gels were soaked in transfer buffer (20% methanol/0.15 M glycine/0.02 M Tris) for 20 min. The proteins were then transferred onto nitrocellulose at 150 V for 1 h. After 1 h incubation in blocking buffer (4% nonfat dry milk in wash buffer [0.15 M NaCl/0.01 M Tris, pH 7.4]), the nitrocellulose was probed with antibodies (20 μg –2 mg in blocking buffer) for at least 2 h. The nitrocellulose was washed with 0.05% NP-40 in

wash buffer (4×50 mL for 1 h) and then probed with anti-rabbit IgG for 2 h. After the blot was washed for 1 h in 0.05% NP-40/wash buffer (4×50 mL), IgG was detected with incubation in 20 mL of NBT, BCIP, 0.1 M NaCl, 5 mM MgCl_2 , and Tris, pH 9.5.

Immunoaffinity Purification of CIC-0. Anti-CIC-0 immunoaffinity columns were constructed by immobilizing purified anti-CIC-0 antibodies (0.2–1.0 mg) onto Pierce SulfoLink gel using the procedure provided by Pierce.

Torpedo membrane proteins were solubilized with 25 mM CHAPS (unless otherwise noted) in buffer 1 (125 mM NaCl, 25 mM KCl, 10 mM glutamic acid, 0.5 mM EGTA, and 20 mM Tris-HCl, pH 7.6) as described previously (Middleton et al., 1994). The immunoaffinity column (1 mL) was washed with 10 mL of buffer 2 (15 mM CHAPS, 1 mg/mL lipid mix in buffer 1). Solubilized protein (0.3–4.7 mg) was incubated with immunoaffinity resin for 30 min. For analytical experiments, 0.3 mL of extract was applied to the column; for preparative experiments, the column matrix was mixed with extract (1.5–3.5 mL). The flow-through in each case consisted of any excess liquid drained from the column and the first 2 mL of wash. The column was further washed with 5 mL of buffer 2 and then with 5 mL of 0.1% Triton X-114 and 0.2 mg/mL lipid mix in buffer 1 (unless otherwise noted), followed by 5 mL of buffer 2. The column was incubated for 45 min with 1 mL of a synthetic peptide (0.2 mM in buffer 2) corresponding to the 19 residues beginning at Glu-646 of the *Torpedo californica* sequence (O'Neill et al., 1991). CIC-0 was then eluted with addition of another 1.5 mL of peptide. All steps were done at 4 °C. Proteins in each sample (0.1–1.0 μg) were separated by electrophoresis on 7.5% acrylamide SDS-PAGE gels and visualized by silver-staining as described above.

Concentrative Uptake of $^{36}\text{Cl}^-$. Samples were reconstituted into liposomes for analysis of $^{36}\text{Cl}^-$ concentrative uptake as described previously (Goldberg & Miller, 1991; Middleton et al., 1994). Briefly, crude extract (5 μg), flow-through (5 μg), and purified Cl^- channel (0.2–1.0 μg) were incubated in 100 μL of 1 mg of lipid mix/15 mM CHAPS in buffer 1 on ice for 20 min. Proteins were reconstituted into liposomes after rapid removal of CHAPS by centrifuging samples through 1.5 mL Sephadex G-50 columns. Liposomes were then centrifuged through G-50 Sephadex into a Cl^- -free buffer (125 mM sodium-glutamate, 25 mM potassium glutamate, 10 mM glutamic acid, and 20 mM Tris-glutamate, pH 7.6) to remove external Cl^- , and $^{36}\text{Cl}^-$ (1.4 mM HCl) was added. After 20 min, aliquots were passed over 1.5 mL Dowex columns to remove free $^{36}\text{Cl}^-$, and the liposome-trapped $^{36}\text{Cl}^-$ was determined by scintillation counting.

Planar Bilayer Measurements. Direct electrical observations in planar lipid bilayers were used to confirm the abundance of active Cl^- channels predicted by $^{36}\text{Cl}^-$ uptake and to compare the functional properties of the purified Cl^- channel to previously published results (Miller & Richard, 1990). The planar lipid bilayer system was as described previously (Middleton et al., 1994), and channel records were filtered at 300–1000 Hz. In order to determine the abundance of active Cl^- channels, the nystatin-induced liposome fusion method was used (Woodbury & Miller, 1990). Briefly, purified CIC-0 (0.2–2 μg) was reconstituted into liposomes as described above except that the lipid mix (0.2 mg) contained ergosterol instead of cholesterol. Lip-

osomes were stored in 150 μL aliquots at -70 °C for up to 2 weeks. Before use, liposomes were thawed, and a freshly prepared nystatin solution was added (50 $\mu\text{g}/\text{mL}$, final concentration). Liposomes sonicated 2×3 s in a bath sonicator (20–50 μL) were added to the cis chamber (450 mM NaCl/10 mM HEPES, pH 7.4) with stirring. The trans chamber contained 150 mM NaCl/10 mM HEPES, pH 7.4. A holding voltage (typically -50 mV) was applied, and current was monitored for “spikes” of anionic conductance indicative of liposome fusions. Some liposome fusions resulted in the insertion of an active Cl^- channel(s) into the lipid bilayer. Therefore, it was possible to determine the number of active Cl^- channels present in a given number of liposomes. By convention, the trans chamber is defined as zero voltage.

V8 Proteolytic Digestion. We used V8 protease for partial digestion of CIC-0 in SDS-PAGE gels because it remains active in SDS. V8 protease cleaves on the C-terminal side of either aspartate or glutamate residues. Purified CIC-0 (0.1 mg/mL) was concentrated and desalted as described below for the Pierce BCA protein assay. The samples were adjusted to 1.0% SDS and then incubated overnight at room temperature with or without 0.002 unit of endoglycosidase H. Aliquots (≈ 2 μg) were solubilized in Laemmli loading buffer, and V8 protease was added (0, 0.1, or 1.0 μg) just prior to loading samples onto the gels. Two 12% acrylamide SDS-PAGE gels were run in parallel, each with half of the sample. Once the tracking dye had reached the running gel (≈ 30 min), the gels were stopped for 30 min to allow proteolysis to proceed. The gels were then restarted to separate the proteolytic fragments. One gel was silver-stained, and the other was transferred to nitrocellulose and probed with 140 μg of pure anti-CIC-0 antibody as described above.

Sucrose Density Gradients. Linear gradients (4.7 mL) of 25–5% sucrose (w/v) in 25 mM CHAPS/1 mg/mL lipid mix in buffer 1 were formed in Beckman SW 50.1 tubes. In order to convert dimer AChR to its monomer form (Sobel et al., 1977), a portion of the crude CHAPS extract (47 μL) was treated with 15 mM mercaptoethanol for 30 min (on ice) prior to loading onto a gradient that contained 15 mM mercaptoethanol. Gradients were loaded with 385 μL of pure CIC-0 (≈ 5 μg) that was doped with 15 μL of crude extract (≈ 15 μg). Gradients were centrifuged at 35 000 rpm for 16 h, and 15 fractions (14 drops, ≈ 300 μL) were collected from the bottom of the tube. Aliquots (20 μL) were analyzed on 7.5% acrylamide SDS-PAGE gels, and the proteins were visualized with silver-staining. Sedimentation coefficients were estimated from the radial distance traveled in a $\omega^2 t$ of $7.7 \times 10^{11} \text{ s}^{-1}$. Sedimentation coefficients were converted to $s_{20,w}$ by using the density and viscosity of the sucrose present at half the radial distance traveled.

Protein Sequence Analysis. Automated Edman degradation was performed by the HHMI Biopolymers facilities at Harvard Medical School. Purified CIC-0 (≈ 100 pmol) was concentrated and chromatographed on Sephadex G-50 (in 15 mM CHAPS/PBS) as described below for the Pierce BCA protein assay. The sample (110 μL) was spun in an Applied Biosystems ProSpin cartridge onto a PVDF membrane. The membrane was washed 2 times with 40 μL of 20% methanol by spinning in the cartridge. The membrane was then removed and washed 8 times by vortexing in 1 mL of 20% methanol. The membrane was then submitted to sequential Edman degradation.

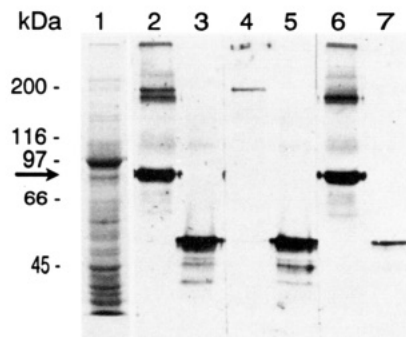


FIGURE 1: Identification of the CIC-0 protein in *Torpedo* electrocyte membranes using affinity-purified anti-CIC-0 antibodies. CIC-0-rich electrocyte membranes (40 μ g, lanes 1, 2, 4, 6) and fusion protein (0.03 μ g, lanes 3, 5, 7) were run on a 7.5% acrylamide SDS-PAGE gel. Protein was stained with Coomassie blue (lane 1) or transferred to nitrocellulose (lanes 2–7). The nitrocellulose was probed with either serum (200 μ L, lanes 2, 3) or serum after passing through the peptide affinity column (1.0 mL, lanes 4, 5), or affinity-purified antibodies (20 μ g, lanes 6, 7). The arrow shows the position of CIC-0. Molecular mass standards were myosin (200 kDa), β -galactosidase (116 kDa), phosphorylase B (97 kDa), bovine albumin (66 kDa), and ovalbumin (45 kDa).

Protein Assays. In order to assay purified CIC-0 for protein, it was necessary to remove the peptide used to elute CIC-0. This was accomplished in two ways. Samples were reconstituted as if to be assayed for $^{36}\text{Cl}^-$ uptake, and various volumes (≈ 100 –400 μ L) were assayed after TCA precipitation (Schaffner & Weismann, 1973). Samples were also assayed by the Pierce BCA protein assay. However, the high concentrations of lipid mix used for reconstitution interfered with this assay. Instead, samples were concentrated ≈ 25 -fold with a Centricon-100 concentrator (Amicon). The concentrated CIC-0 was then chromatographed on a 0.75 mL G-50 Sephadex column (equilibrated with 15 mM CHAPS in buffer 1) to remove the lipid mix, any excess CHAPS, and the peptide used for elution.

RESULTS

As a first step toward the purification of CIC-0, anti-CIC-0 antiserum was used to identify the CIC-0 protein in membrane preparations from *Torpedo californica* electric organs. A fusion protein consisting of the first 314 residues of phage T7 gene-9 followed by 18 residues of *T. marmorata* CIC-0 (E-642 to P-659; Jentsch et al., 1990) was used to generate anti-CIC-0 antiserum in rabbits. *Torpedo* electrocyte membrane proteins were transferred to nitrocellulose and probed with anti-CIC-0 antiserum (Figure 1). The serum recognizes a 90-kDa polypeptide that corresponds to a polypeptide migrating slightly ahead of the principal band in our membrane preparation, the α -subunit of the Na/K-ATPase (Figure 1, lanes 1, 2). An apparent molecular mass of 90 kDa is consistent with the 89-kDa value expected for the protein portion of CIC-0 from *T. californica* (O'Neill et al., 1991).

We purified CIC-0-specific antibodies from anti-CIC-0 antiserum using a peptide affinity column. The purification of CIC-0-specific antibodies was monitored by probing a Western blot that compared CIC-0-rich membranes with the T7 gene-9 fusion protein antigen (Figure 1). The affinity column efficiently removes anti-CIC-0 antibodies from the total serum but ignores the antibodies that recognize gene 9 epitopes (Figure 1, lanes 4, 5). Affinity-purified anti-CIC-0

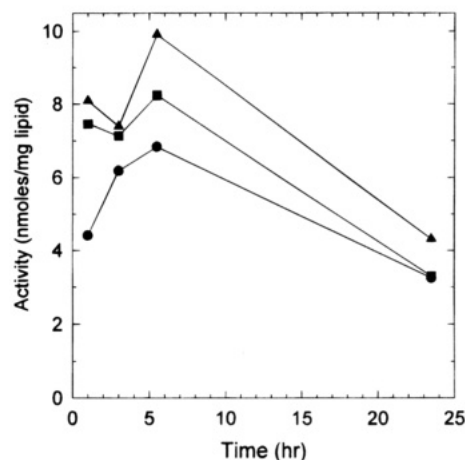


FIGURE 2: Extraction and survival of CIC-0 activity in CHAPS. CIC-0-rich membranes (200 μ g) were solubilized with 15 mM (●), 25 mM (■), or 50 mM (▲) CHAPS. After incubation on ice for the indicated times, the samples were reconstituted into liposomes and assayed for $^{36}\text{Cl}^-$ uptake. Activity is reported as 20 min $^{36}\text{Cl}^-$ uptake.

antibodies at the 20 μ g level (Figure 1, lanes 6, 7) generate a signal equivalent to ≈ 2 mg of antibody in serum. The affinity-purified antibodies were then used to construct anti-CIC-0 immunoaffinity columns.

Immunoaffinity Purification of the *Torpedo* Cl^- Channel. We have shown that CIC-0 can be extracted from *Torpedo* membranes into the detergent CHAPS and assayed for function by uptake of $^{36}\text{Cl}^-$ after reconstitution into liposomes (Middleton et al., 1994). Figure 2 shows that CIC-0 remains active in CHAPS for at least 5 h on ice. About 50% of the $^{36}\text{Cl}^-$ uptake activity initially in crude extract is lost after 24 h. A slight increase in uptake activity (10–50%) is observed during the first 5 h incubation with CHAPS. Increased dispersal in CHAPS micelles of initially aggregated channels may account for this increased uptake. The stability of CIC-0 in CHAPS makes it possible to purify active channels using procedures completed in 1 day.

Anti-CIC-0 immunoaffinity columns were used to purify CIC-0 from CHAPS extracts of *Torpedo* membranes (Figure 3). CIC-0 (90-kDa band) bound efficiently to these affinity columns, as is seen in silver-stained gels (Figure 3, lanes 1 vs 2 and 3) and Western blots (data not shown). CIC-0 could be eluted with a peptide containing the CIC-0 sequence used to raise the antibodies (Figure 3, lane 4). Quite unexpectedly, two other polypeptides reproducibly coeluted with CIC-0. N-Terminal sequence analysis of these other two proteins (data not shown) revealed that the 97- and 105-kDa polypeptides were the α -subunit of the Na/K-ATPase (Kawakami et al., 1985) and the SITS-binding protein (Jentsch et al., 1989), respectively. When the column was washed with 0.1% Triton X-114 prior to eluting CIC-0, however, these two polypeptides were specifically removed (data not shown), and CIC-0 was eluted free of these contaminants (Figure 3, lane 5).

The nature of the interaction of CIC-0 with the Na/K-ATPase and SITS-binding protein was examined in some detail. In contrast to CIC-0, only a small fraction of these two polypeptides bind to the anti-CIC-0 immunoaffinity column (data not shown). Two lines of evidence suggest that these two polypeptides associate with CIC-0 through hydrophobic interactions. First, the Na/K-ATPase and SITS-

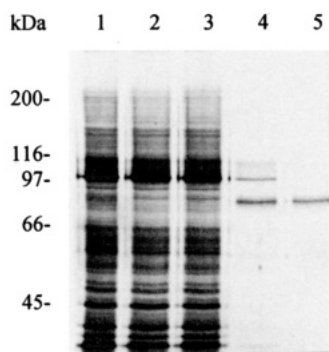


FIGURE 3: Purification of CIC-0 by immunoaffinity chromatography. Crude CHAPS extract of CIC-0-rich membranes (lane 1) was incubated with two batches (1 mL) of anti-CIC-0 immunoaffinity resin, and the material not bound to the resin was washed off (lanes 2, 3). One column was also washed with 0.1% Triton X-114 (lanes 3, 5). Bound protein was eluted with peptide from both the column not washed (lane 4) and the column washed (lane 5) with 0.1% Triton X-114. Samples were separated on a 7.5% acrylamide SDS-PAGE gel and visualized by silver-staining. Samples in lanes 4 and 5 were balanced to contain the same amount of channel activity, based on uptake of $^{36}\text{Cl}^-$.

binding protein remain associated with CIC-0 in high salt (600 mM NaCl). Second, the efficiency with which the family of polyoxyethylene detergents release these two polypeptides from the column (Triton-X114 > NP-40 > Triton X-100 >> Triton X-405) correlates with the solubilizing power of these detergents (Slinde & Flatmark, 1976).

The binding and recovery of active CIC-0 were determined by the uptake of $^{36}\text{Cl}^-$ into reconstituted proteoliposomes. For the experiment shown in Figure 3, one column bound 60% (lanes 2, 4) and the other bound 80% of the activity (lanes 3, 5) present in crude extract. About half the column-bound activity could be eluted with peptide. The remaining CIC-0 could be removed by washing the column with a low-pH buffer (0.1 M glycine, pH 3.0), and this qualitatively accounts for the unrecovered Cl^- channel activity (data not shown). Most importantly, removal of the Na/K-ATPase and SITS-binding protein with Triton X-114 did not affect the activity of CIC-0. Lanes 4 and 5 of Figure 3 compare two preparations, with and without the Triton wash step, in which the same Cl^- uptake activity was applied to each lane. These two preparations contained similar amounts of CIC-0 protein but differed greatly in the two other polypeptides.

In order to quantify the recovery of pure CIC-0 protein, larger amounts (1.5–3.5 mL) of crude CHAPS extract were used. The results from six separate experiments using the same batch of immunoaffinity resin (1 mL) are shown in Table 1. In each experiment, the column was washed with 0.1% Triton X-114 before elution of CIC-0. On average, $\approx 70\%$ of the $^{36}\text{Cl}^-$ uptake activity bound to the column, and $\approx 20\%$ of the bound activity was eluted with peptide (Table 1). A substantial amount of CIC-0 was recovered after washing the column with a low-pH buffer and qualitatively accounted for the remaining activity (data not shown).

We encountered two difficulties when measuring the protein eluted with the peptide. CIC-0 is recovered in a dilute solution (≈ 0.01 mg/ml) and in the presence of a high concentration of peptide. Two different protein assays were used. In the first three experiments (Table 1), CIC-0 was incorporated into liposomes, which were subsequently separated from the aqueous peptide. A TCA precipitation assay (Schaffner & Weismann, 1973) was then used to measure

Table 1: Quantitative Analysis of the Purification of CIC-0^a

sample	prepn	volume (mL)	protein ^b (mg)	act. ^c ($\mu\text{mol}/\text{mg}$ of lipid)	sp act. ^d	purification
extract	1	1.5	1.1	2.20	2.0	1.0
	2	2.5	1.6	3.32	2.1	1.0
	3	2.5	1.5	1.71	1.1	1.0
	4	1.8	1.9	2.35	1.2	1.0
	5	1.8	3.1	3.38	1.1	1.0
	6	3.5	4.7	13.40	2.9	1.0
flow-through	1	3.5	1.2	0.51	0.42	0.21
	2	4.5	1.8	0.94	0.52	0.25
	3	4.5	1.4	0.61	0.44	0.40
	4	3.8	2.1	0.53	0.25	0.21
	5	3.8	2.9	1.08	0.37	0.34
	6	5.5	3.7	4.97	1.34	0.46
pure channel	1	1.5	0.0045	0.33	73.3	36.7
	2	1.5	0.0045	0.36	80.0	38.1
	3	1.5	0.0052	0.27	51.9	47.2
	4	1.5	0.018	0.31	17.2	14.3
	5	1.5	0.021	0.42	20.0	18.2
	6	1.5	0.041	1.36	33.2	11.4

^a Six separate purification experiments were analyzed. Crude extract, flow-through, and pure CIC-0 were assayed for protein and $^{36}\text{Cl}^-$ uptake.

^b Protein was assayed after reconstitution by a TCA precipitation assay for preparations 1–3 and was assayed with the Pierce BCA assay after concentration and desalting for preparations 4–6. ^c Cl^- channels were assayed by concentrative uptake of $^{36}\text{Cl}^-$. ^d Specific activity is micro-moles per milligram of lipid per milligram of protein.

the lipid-associated protein. However, the signal obtained was low and only slightly higher than the background contributed by the lipid.

In the second set of experiments (Table 1, preparations 4–6), the BCA protein assay was used after removal of lipid and peptide by gel filtration. Since this procedure leads to losses in protein, these values represent a minimum estimate of protein recovery. However, the BCA assay estimated a protein recovery 4 times larger than the TCA precipitation assay. Therefore, when the TCA assay was used, a purification of ≈ 40 -fold was calculated whereas the BCA assay estimated ≈ 15 -fold purification. This indicates that 2.5–7% of the total protein in our membrane preparation is CIC-0 protein, consistent with previous estimates of channel abundance (Goldberg & Miller, 1991).

To confirm that the material eluted with peptide consisted only of CIC-0, a sample was submitted to N-terminal sequence analysis. Automated Edman degradation revealed a sequence (Table 2) which begins at Ser-2 of the predicted sequence of CIC-0 from *Torpedo californica* (O'Neill et al., 1991). No other residues were apparent in the 10 cycles analyzed.

Analysis of the Functional Properties of Purified CIC-0. We appraised the functional behavior of purified CIC-0 by direct electrical recording of single channels. The method for controlled, reliable fusion of CIC-0-reconstituted proteoliposomes into planar lipid bilayers has been described in detail (Middleton et al., 1994). As shown in Figure 4, the purified channels open with bursts of activity separated by long-lived "inactivated intervals", as originally described for channels from native membrane vesicles (Miller, 1982). During the bursts, channels rapidly fluctuate among three equally spaced conductance levels, a zero-current level and two conducting states that reflect the opening of one or both of the two protochannels making up the conducting unit (Miller, 1982; Hanke & Miller, 1983). Depolarization favors

Table 2: Sequence Analysis of Purified ClC-0^a

CIC-0 ^b	cycle	amino acid	pmol ^c
Met			
Ser	1	Ser	12.9
His	2	His	1.2
Glu	3	Glu	2.5
Lys	4	Lys	2.8
Asn	5	Asn (Asp)	1.3 (1.5)
Glu	6	Glu	1.3
Ala	7	Ala	1.6
Ser	8	Ser	2.8
Gly	9	Gly	0.8
Asn	10	Asn	1.2

^a Purified ClC-0 (≈ 100 pmol) was concentrated, desalted, and submitted to automated Edman degradation as described under Materials and Methods. ^b The sequence predicted from the cDNA encoding *Torpedo californica* ClC-0 (O'Neill et al., 1991). ^c The quantity released was determined from the rise in amino acid over the previous cycle, except for cycle 1.

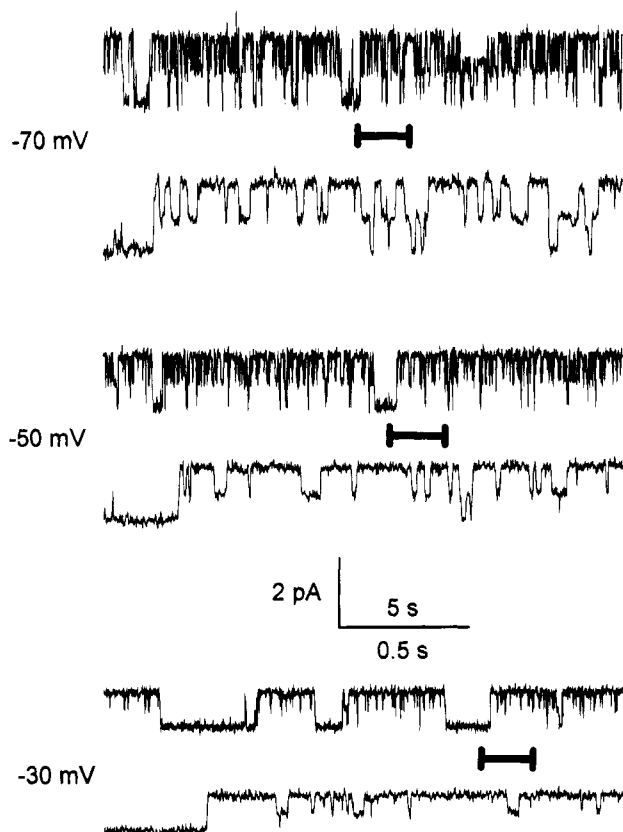


FIGURE 4: Single-channel records of purified ClC-0. Purified ClC-0 was reconstituted into a planar lipid bilayer with 450 mM Cl⁻ on the cis side and 150 mM Cl⁻ on the trans side of the bilayer. Recordings are shown at -70, -50, and -30 mV, at low time resolution (upper traces), or at an expanded time-scale (lower traces, data taken from intervals marked by dark bars).

channel opening within the burst, and hence the appearance of the higher conductance levels, as is apparent from the raw channel records. In addition, the figure illustrates the increased probability of inactivation events at more depolarized potentials.

The voltage dependence of channel behavior was quantified for comparison with channels from native membranes (Figure 5). In symmetrical 150 mM Cl⁻, the current through both open states is a linear function of voltage from -150 to 80 mV (Figure 5A). Across the range of holding potentials, the largest conductance was always twice the

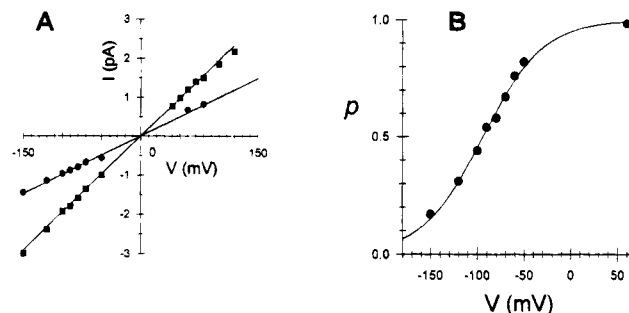


FIGURE 5: Voltage dependence of purified ClC-0. A single purified Cl⁻ channel was fused into a planar lipid bilayer with symmetrical 150 mM NaCl. The current through each conductance level was measured at various voltages (A) and fit to lines with slopes of 9.9 pS (●) and 19.4 pS (■) for the middle and upper conductance levels, respectively. The probability of channel opening was measured at various voltages (B) and fit to the equation $p(V) = [1 + \exp(1 - zF(V - V_0)/RT)]^{-1}$ with $V_0 = -94$ mV and $z = 0.79$.

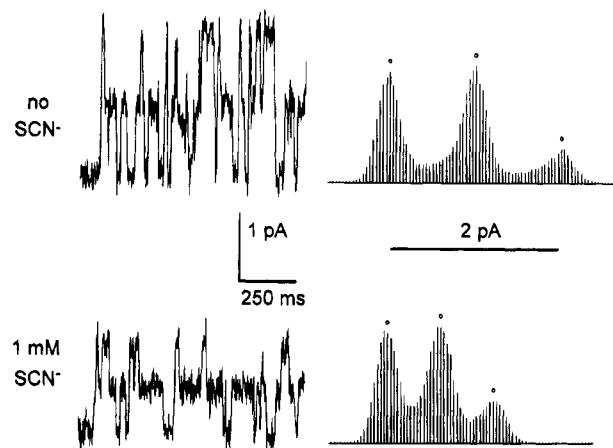


FIGURE 6: SCN⁻ block of purified ClC-0. Purified ClC-0 was reconstituted into a planar lipid bilayer with symmetrical 150 mM Cl⁻. The upper and lower traces show 1 s of channel activity at -100 mV in the absence and presence of 1 mM NaSCN. Next to each trace are current amplitude histograms which were compiled from 73 s (upper) and 40 s (lower) of recording in the absence and presence of 1 mM NaSCN, respectively. The middle level current was 1.04 and 0.64 pA, and the upper level current was 2.08 and 1.28 pA in the absence and presence of NaSCN, respectively.

middle conductance (approximately 10 and 20 pS), as expected for two identical pores. Within a burst event, the probability of channel opening increased with depolarization (Figure 5B), with half-saturation voltage of -94 mV, consistent with previous measurements (Miller, 1982; Hanke & Miller, 1983).

These results show that both conduction and gating properties are preserved in the purified ClC-0 channel. In addition, SCN⁻ is known to block the *Torpedo* Cl⁻ channel in a reversible and voltage-dependent manner with a K_i at -100 mV of 2 mM (White & Miller, 1981). Figure 6 shows that rapid, reversible SCN⁻ block is recapitulated in the purified channel where the current is reduced 40% in the presence of 1 mM SCN⁻ at -100 mV. This result further substantiates the functional integrity of the purified Cl⁻ channel.

It is worth noting that the probability of observing inactivation events varied from channel to channel. Many channels behaved qualitatively as previously reported (Miller, 1982); however, some inactivated infrequently, even at strong depolarizing potentials. All channels eventually inactivated

Table 3: Analysis of Cl⁻ Channel Abundance^a

prepn	act. reconstituted ^b	nystatin spikes obsd	Cl ⁻ channels obsd	channels/ spike
1	17.7	114	8	0.07
2	9.6	152	24	0.17
3	22.5	80	9	0.11
4	72.7	239	65	0.27

^a Purified CIC-0 from four independent experiments was reconstituted into liposomes (0.2 mg) for analysis by nystatin-induced liposome fusion into planar lipid bilayers. Several reconstitution samples (3–6) were analyzed from each preparation. ^b The amount of active Cl⁻ channel present in each reconstitution sample as determined by the uptake of ³⁶Cl⁻ (nmoles per milligram of lipid).

when submitted to long depolarizing potentials (many minutes). Further studies are necessary to determine the source of this variation.

Abundance of Active Channels in Purified Preparations. The mere observation of single-channel activity in a biochemical preparation does not by itself make a compelling case for the functional competence of the preparation. The channels actually observed in a planar bilayer experiment represent only a minuscule fraction ($<10^{-10}$) of the protein present in the experimental system, and could, in principle, reflect a vanishingly small amount of active material in a largely denatured collection of channel molecules. For this reason, it is essential to know to what extent the single channels observed are representative of the whole population in the proteoliposomes. We used the “nystatin-spike” method (Woodbury & Miller, 1990) in order to attack this question. Here, nystatin, a pore-forming antibiotic, is uniformly incorporated into the CIC-0 proteoliposomes, a maneuver that renders all liposomes capable of fusing into the planar bilayer. Each liposome fusion event is detected as a transient “spike” of nystatin-mediated conductance. The method thus allows distinction between liposomes containing CIC-0 channels from those devoid of CIC-0 and provides an assay of the fraction of liposomes that carry active CIC-0 channels (Middleton et al., 1994).

Table 3 presents the result of such channel-abundance assays on 4 separate preparations of purified, reconstituted CIC-0, which collected over 500 fusion events in total. The total number of Cl⁻ channels observed was 7–27% of the number of liposome fusions detected. In each preparation, about half of the channels observed were from liposomes containing two channels, an unexpected result if CIC-0 distributes uniformly among the liposomes. In fact, in the preparation with the highest amount of ³⁶Cl⁻ activity (Table 3, preparation 4), many liposomes contained three or more Cl⁻ channels. This result suggests that channels aggregate within the large freeze/thaw liposomes and remain clustered when liposomes are decreased in size by sonication. We note with surprise that almost all channels inserted into bilayers asymmetrically, with the extracellular side facing the trans chamber, as is also observed for native *Torpedo* membranes (Miller & Richard, 1990).

How do we determine how many liposomes should have Cl⁻ channels? Unfortunately, this number is critically dependent on liposome diameter, which in our preparations varies widely from 200 to 5000 Å (Carter-Su et al., 1980). We assume that the liposomes may be approximated by a uniform population of 1000-Å diameter spheres and that the molecular mass of an active channel is 200 kDa (see below).

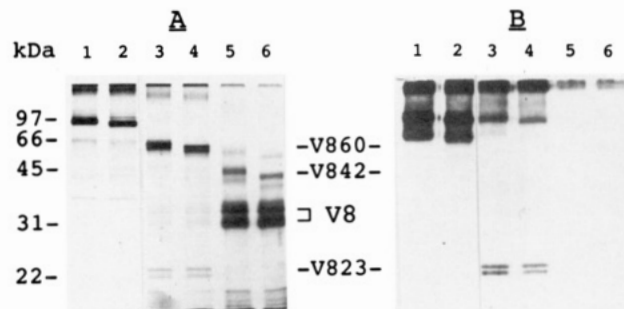


FIGURE 7: Identification of the site for Asn-linked glycosylation. Purified CIC-0 was digested with (lanes 2, 4, 6) or without (lanes 1, 3, 5) endoglycosidase H. Samples were solubilized in Laemmli load buffer and had 0 (lanes 1, 2), 0.1 μ g (lanes 3, 4), or 1 μ g (lanes 5, 6) of V8 protease added. Samples were immediately loaded onto two 12% acrylamide SDS-PAGE gels. After electrophoresis, proteins were either visualized by silver-stain (A) or transferred to nitrocellulose and probed with 140 μ g of purified anti-CIC-0 antibody (B). Molecular mass standards were the same as in Figure 1 with the addition of carbonic anhydrase (31 kDa) and soybean trypsin inhibitor (22 kDa).

Then, in a typical reconstitution mixture containing 200 μ g of lipid and $\approx 1 \mu$ g of CIC-0, there should be 2×10^{12} liposomes and $(1-5) \times 10^{12}$ channels (depending on the protein assay used), i.e., about the same number of channels as liposomes. The observed channel abundance falls about 10-fold below this expectation (Table 3). However, if the liposomes were smaller than assumed above, 300 Å in diameter, the expected and observed channel abundances would agree precisely. We consider this rough agreement as an excellent indication that the channels we observe in the planar bilayers represent the overall channel population in the preparation, and not a minor fraction of uncharacteristically healthy channels. This conclusion is in harmony with the excellent recovery of Cl⁻ flux activity, which, though of low functional resolution, is representative of the bulk population of channel protein.

Identification of the Site for Asn-Linked Oligosaccharide. CIC-0 from *Torpedo californica* has two potential sites for Asn-linked oligosaccharide located at residues 365 and 806. Digestion of purified CIC-0 with either endoglycosidase H (Figure 7, lane 2) or N-glycanase (data not shown) results in the same ≈ 2 kDa decrease in apparent molecular mass. On the basis of this small mobility shift and known glycosidase specificity (Kornfield & Kornfield, 1985; Maley et al., 1989), these results suggest that only one Asn residue is glycosylated with high mannose-type oligosaccharide.

In order to identify the glycosylated region of the channel, we cleaved purified CIC-0 with V8 protease before or after removal of Asn-linked oligosaccharide. Proteolytic fragments were identified both by protein staining (Figure 7A) and by immunoblotting (Figure 7B) with antibodies that recognize an epitope located between the two possible Asn-linked glycosylation sites ≈ 160 residues from the C-terminus. Mild digestion with V8 protease produces a ≈ 60 -kDa fragment containing oligosaccharide and a ≈ 23 -kDa doublet free of oligosaccharide (Figure 7, lanes 3, 4). Since the 23-kDa doublet is recognized by the anti-CIC-0 antibody, it is a C-terminal fragment. Conversely, the 60-kDa fragment is not recognized by our antibody and is therefore an N-terminal fragment. Overdigestion with V8 protease results in a 42-kDa fragment which clearly contains oligosaccharide but is not recognized by our antibody. This 42-kDa fragment

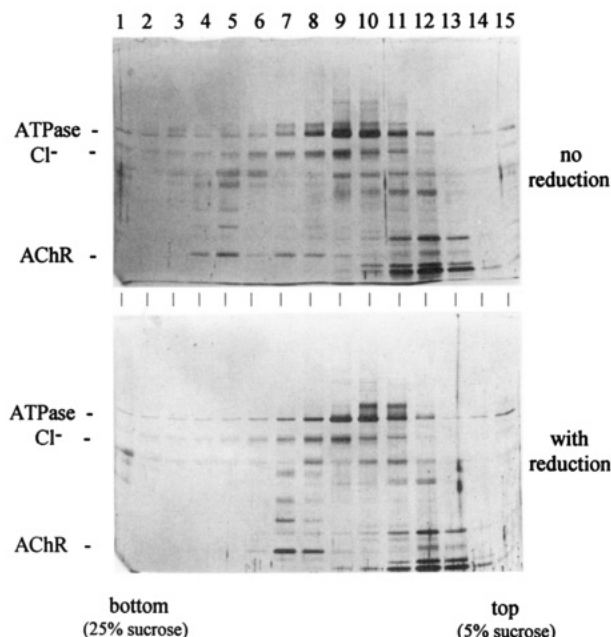


FIGURE 8: Molecular mass estimation of purified CIC-0 by velocity sedimentation. Purified CIC-0 ($\approx 5 \mu\text{g}$) and crude extract ($\approx 15 \mu\text{g}$) were combined and loaded onto two linear sucrose gradients (5–25%) in the absence (upper panel) or presence (lower panel) of 15 mM mercaptoethanol. After centrifugation for 16 h, 15 fractions ($\approx 300 \mu\text{L}$) were collected from the bottom of each tube. Aliquots ($20 \mu\text{L}$) were run on 7.5% acrylamide SDS–PAGE gels and the proteins visualized by silver-stain. The positions of the α -subunit of the Na/K-ATPase (ATPase), CIC-0 (Cl^-), and the α -subunit of the AChR (AChR) are marked.

cannot include Asn-806, since the largest possible fragment which both contains Asn-806 and excludes our epitope would be ≈ 20 kDa. Therefore, Asn-365 must be the site for glycosylation in both the 60-kDa and 42-kDa fragments. We cannot rule out the possibility that Asn-806 is also glycosylated, but both the V8-60 and V8-42 fragments appear to account for all 2 kDa of oligosaccharide present in CIC-0. This conclusion is in harmony with recent *in vitro* translation studies of a CIC-0 homologue (Kieferle et al., 1994), in which the equivalent residue was found to be glycosylated.

Estimation of the Molecular Mass of Intact CIC-0. The molecular mass of purified CIC-0 was estimated by sedimentation in sucrose density gradients under conditions which preserve channel activity. Two well-characterized membrane transport proteins, the Na/K-ATPase and the nicotinic acetylcholine receptor (AChR), were used as molecular mass standards. The smallest and most abundant form of the Na/K-ATPase in detergent solutions is the α/β -protomer of molecular mass ≈ 150 kDa (Hayashi et al., 1983; Esmann, 1988). The *Torpedo* AChR exists in two forms, a disulfide-linked dimer of ≈ 600 kDa and a monomer of ≈ 300 kDa (Popot & Changeux, 1984).

Purified CIC-0 and crude extract containing the molecular mass standards were mixed, and the samples were centrifuged overnight in sucrose gradients (5–25%) under reducing or oxidizing conditions (Figure 8). AChR dimers are located primarily in fractions 4 and 5 (Figure 8, upper panel) and sediment with an $s_{20,w}$ of ≈ 13 S, while monomer AChR appears in fractions 7 and 8 (Figure 8, lower panel) and sediments at ≈ 9 S, in excellent agreement with values determined more precisely in the analytical ultracentrifuge (Reynolds & Karlin, 1978). The Na/K-ATPase sediments more slowly, appearing primarily in fractions 9 and 10 under

both oxidizing and reducing conditions (≈ 6 S). The identity of these bands was confirmed with antibodies specific to the α -subunits of both the AChR and the Na/K-ATPase (data not shown). With both oxidizing and reducing conditions, purified CIC-0 is primarily detected in fraction 9 (≈ 7 S), clearly between the 300-kDa and 150-kDa standards. Since CIC-0 runs just slightly ahead of the Na/K-ATPase, we estimate its molecular mass at ≈ 200 kDa. We therefore propose the active, double-barreled, CIC-0 channel is formed as a homodimer of the 90-kDa polypeptide purified here.

DISCUSSION

We have developed a one-step immunoaffinity purification procedure to isolate functional *Torpedo* Cl^- channels. N-terminal sequence analysis confirms that we have purified CIC-0, the Cl^- channel cloned from *Torpedo* electroplax (Jentsch et al., 1990). Consistent with expression studies of CIC-0 in oocytes (Bauer et al., 1991), a single polypeptide species is sufficient for construction of a fully functional “double-barreled” Cl^- channel. No auxiliary subunits are associated with CIC-0, in contrast to Ca^{2+} , Na^+ , and K^+ channels, which when purified from natural sources are tightly associated with nonhomologous subunits (Isom et al., 1994). Our initial purification results found two other polypeptides associated with CIC-0, but only a minor fraction of these polypeptides (Na/K-ATPase and SITS-binding protein) copurified with CIC-0. Moreover, fully active channels were recovered after removal of these associated polypeptides, which are thus likely to be nonspecifically associated with CIC-0 in the detergent extract. Nonspecific association may also explain the recent erroneous suggestion that the *Torpedo* Cl^- channel is composed of four different polypeptides (Rosenthal & Guidotti, 1994).

Purified Cl^- channels were fully functional, as judged by two criteria. First, uptake of $^{36}\text{Cl}^-$ showed that 20–60% of the activity bound to the affinity column could be eluted with peptide. Second, estimates of Cl^- channel abundance in planar lipid bilayers are qualitatively consistent with the expected number of purified active channels. In our screening of more than 100 purified single channels, all displayed the expected “double-barreled” gating behavior.

The *Torpedo* Cl^- channel has two potential Asn-linked glycosylation sites (Jentsch et al., 1990), but only one (equivalent to Asn-365) is conserved in other tissues (Steinmeyer et al., 1991; Uchida et al., 1993; Theimann et al., 1992). In addition, a homologue abundantly expressed in brain (Kawasaki et al., 1994) has 2 potential glycosylation sites located within 16 residues of the conserved Asn. We have now demonstrated that CIC-0 is indeed glycosylated at this conserved residue. In the current model for the transmembrane topology of CIC-0, this glycosylation occurs between the predicted transmembrane domains 8 and 9 (Figure 9A), on the cytoplasmic side of the membrane. Since glycosylation nearly always occurs on the extracellular portion of membrane proteins (Kornfield & Kornfield, 1985) the current model (Figure 9A) of CIC-0 transmembrane topology is probably incorrect.

By direct protein sequencing, we have confirmed that CIC-0 does not contain a cleavable signal sequence. Since the N-terminus is highly charged, it is unlikely to be transported across the membrane. Therefore, the N-terminus is probably located in the cytoplasm as previously predicted

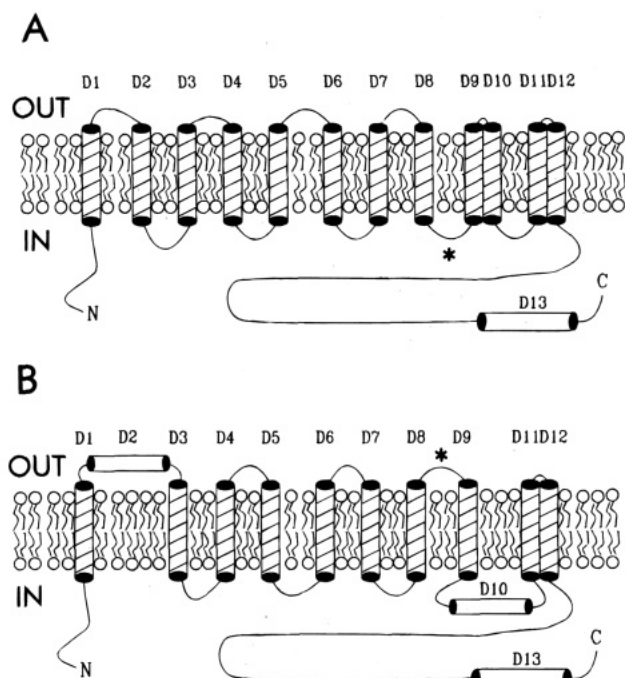


FIGURE 9: Proposed membrane topology for CIC-0. (A) Original topology proposed on the basis of hydrophobicity analysis (Jentsch et al., 1990) (B) A possible model which would place the glycosylated Asn-365 (asterisk) on the extracellular face of the membrane.

(Jentsch et al., 1990). An odd number of transmembrane domains must therefore exist between the N-terminus and the glycosylation site at Asn-365. One member of the CIC family (CIC-K2S) has the predicted transmembrane domain D2 deleted yet still forms functional Cl^- channels in oocytes (Adachi et al., 1994). It therefore is probable that D2 is not a transmembrane domain in CIC-0. Elimination of D2 as a transmembrane domain in the current model (Figure 9A) would place Asn-365 on the extracellular side of the membrane (Figure 9B).

An additional difficulty in predicting transmembrane topology is encountered on the C-terminal side of Asn-365. There is compelling evidence that the region C-terminal to His-695 of CIC-2 is located on the same side of the membrane as the N-terminus (Gründer et al., 1992). If the N-terminus is indeed located in the cytoplasm, then an odd number of membrane crossings must exist between the glycosylated Asn-365 and the homologous region beginning at Gly-648 of CIC-0. In the current model, four putative transmembrane domains (D9–D12) exist between Asn-365 and Gly-648, and therefore either one of these is not a transmembrane domain or a previously unidentified region also crosses the membrane. We favor the elimination of domain 10 (Figure 9B) since four residues are missing in domain 10 from the homologous channel expressed in kidney (Uchida et al., 1993). Of course, it is possible that this domain (or any other domain) crosses the bilayer twice in a nonhelical structure, as proposed for voltage-gated K^+ channels (Yellen et al., 1991; Hartmann et al., 1991).

We have attempted to estimate the size of the active Cl^- channel by sedimentation in density gradients. We have used as internal standards two membrane proteins, the nicotinic acetylcholine receptor and the Na/K-ATPase, that sediment in a well-behaved manner in the same detergent, CHAPS, that preserves the Cl^- channel's activity. Our results firmly

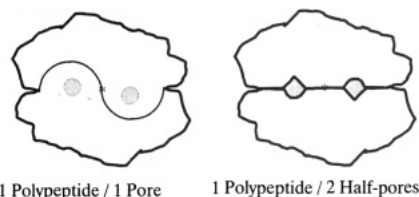


FIGURE 10: Double-barreled channel from a homodimer. Two models for the construction of CIC-0 from two identical subunits. The asterisks mark the centers of 2-fold symmetry.

place CIC-0 close in sedimentation mobility to the Na/K-ATPase (150 kDa) and clearly slower than monomeric AChR (300 kDa). Of course, the hydrodynamic mobility of the Cl^- channel does not by itself rigorously measure its molecular mass. However, we consider it likely that the shape of CIC-0 is similar to the shapes of the internal standards, which are both integral membrane transport proteins. To the extent that this assumption is valid, we conclude that the functional Cl^- channel is a homodimer of the 90-kDa CIC-0 polypeptide. It is also possible that bound detergent may confound our size estimate. However, since quantitative equilibrium centrifugation studies show that the AChR mass is increased only 20% by detergent effects (Reynolds & Karlin, 1978), it is unlikely that CIC-0 can be much larger than ≈ 200 kDa in CHAPS. Since we cannot directly assay channel behavior in micellar solution, it is possible that this 200-kDa particle is not a functional channel, and that the channel is formed as a higher aggregate only after detergent removal and incorporation into a lipid bilayer. This type of assembly of integral membrane channels is without precedent, however.

The "double-barreled" model for CIC-0 predicts that the conducting unit is built from two identical and independently gated protochannels. If CIC-0 is indeed built as a symmetric homodimer, then we can imagine two fundamentally different quaternary architectures (Figure 10). Each protochannel pore could be formed from one subunit. Alternatively, it is possible that each of the subunits contributes to two halves of two protochannel pores. However, since the two pores gate independently, the second model would require part of each subunit to gate without influencing the other pore's gating. On these purely aesthetic grounds, we prefer the model in which each protochannel pore is completely formed from one subunit. This type of molecular architecture is unprecedented among known eukaryotic ion channels, which are built from multiple subunits (or homologous domains) surrounding a central pore.

Our proposal for the dimeric structure of CIC-0 is in apparent conflict with recent molecular genetic studies of CIC-1, a mammalian homologue of CIC-0 (Steinmeyer et al., 1994). Coexpression in *Xenopus* oocytes of wild-type CIC-1 and a point mutant that alters conduction properties at low mixing ratio and disrupts channel formation at higher mixing ratio suggests that the channel complex consists of at least three, and probably four, subunits. We see no simple way to reconcile these conflicting conclusions arising from very different approaches. Since the disposition of polypeptide subunits around the conducting pore is so fundamental to our picture of the channel's structure, we are currently working along both biochemical and molecular genetic lines to resolve this issue.

The analytical-scale purification of CIC-0 raises the possibility of a direct structural attack on the CIC family of

voltage-gated Cl^- channels. The results presented here show that the *Torpedo* electroplax is a natural high-level expression system for CIC-0; we are currently attempting to scale up these procedures to allow 10 mg quantities of the protein to be purified from one *Torpedo* ray. We have hopes that the electroplax-expressed protein may be of good crystallographic quality, since it is only lightly glycosylated and appears to be a homooligomer. Recent advances in techniques of high-resolution electron crystallography (Kühlbrandt, 1992; Unwin, 1993) permit us to view the structure determination of CIC-0 as a practical goal for future work.

ACKNOWLEDGMENT

We thank Dr. Jonathan Cohen for kindly providing the mAb used for detecting the α -subunit of the AChR and Dr. Rock Levinson for encouragement and advice.

REFERENCES

- Adachi, S., Uchida, S., Ito, H., Hata, M., Hiroe, M., Marumo, F., & Sasaki, S. (1994) *J. Biol. Chem.* 269, 17677–17683.
- Bauer, C. K., Steinmeyer, K., Schwarz, J. R., & Jentsch, T. J. (1991) *Proc. Natl. Acad. Sci. U.S.A.* 88, 11052–11056.
- Bryant, S. H. (1973) in *New Developments in Electromyography and Clinical Neurophysiology* (Desmedt, J. E., Ed.) Vol. 1, pp 420–450, S. Karger, Basel.
- Carter-Su, C., Pillion, D. J., & Czech, M. P. (1980) *Biochemistry* 19, 2374–2385.
- Esmann, M. (1988) *Methods Enzymol.* 156, 72–81.
- Finn, A. L., Dillard, M., & Gaido, M. (1993) *Proc. Natl. Acad. Sci. U.S.A.* 90, 5691–5694.
- Franciolini, F., & Petris, A. (1990) *Biochim. Biophys. Acta* 1031, 247–259.
- Goldberg, A. F. X., & Miller, C. (1991) *J. Membr. Biol.* 124, 199–206.
- Gründer, S., Thiemann, A., Pusch, M., & Jentsch, T. J. (1992) *Nature* 360, 759–762.
- Hanke, W., & Miller, C. (1983) *J. Gen. Physiol.* 82, 25–45.
- Hartmann, H. A., Kirsch, G. E., Drewe, J. A., Taglialetela, M., Joho, R. H., & Brown, A. M. (1991) *Science* 251, 942–944.
- Hayashi, Y., Takagi, T., Maezawa, S., & Matsui, H. (1983) *Biochim. Biophys. Acta* 748, 153–167.
- Isom, L. L., De Jongh, K. S., & Catterall, W. A. (1994) *Neuron* 12, 1183–1194.
- Jentsch, T. J., Garcia, A. M., & Lodish, H. F. (1989) *Biochem. J.* 261, 155–166.
- Jentsch, T. J., Steinmeyer, K., & Schwarz, G. (1990) *Nature* 348, 510–514.
- Kawakami, K., Noguchi, S., Noda, M., Takahashi, H., Ohta, T., Kawamura, M., Nojima, H., Nagano, K., Hirose, T., Inayama, S., Hayashida, H., Miyata, T., & Numa, S. (1985) *Nature* 316, 733–736.
- Kawasaki, M., Uchida, S., Monkawa, T., Miyawaki, A., Mikoshiba, K., Marumo, F., & Sasaki, S. (1994) *Neuron* 12, 597–604.
- Kieferle, S., Fong, P., Bens, M., Vandewalle, A., & Jentsch, T. J. (1994) *Proc. Natl. Acad. Sci. U.S.A.* 91, 6943–6947.
- Knaus, H. G., Garcia-Calvo, M., Kaczorowski, G. J., & Garcia, M. L. (1994) *J. Biol. Chem.* 269, 3921–3924.
- Koch, M. C., Steinmeyer, K., Lorenz, C., Ricker, K., Wolf, F., Otto, M., Zoll, B., Lehmann-Horn, F., Grzeschik, K.-H., & Jentsch, T. J. (1992) *Science* 257, 797–800.
- Kornfield, R., & Kornfield, S. (1985) *Annu. Rev. Biochem.* 54, 631–664.
- Kühlbrandt, W. (1992) *Q. Rev. Biophys.* 25, 1–50.
- Laemmli, U. K. (1970) *Nature* 227, 680–685.
- Maley, F., Trimble, R. B., Tarentino, A. L., & Plummer, T. H., Jr. (1989) *Anal. Biochem.* 180, 195–204.
- Merrill, C. R., Goldman, D., Sedman, S. A., & Ebert, M. H. (1981) *Science* 211, 1437–1438.
- Middleton, R. E., Pheasant, D. J., & Miller, C. (1994) *Methods: Compan. Methods Enzymol.* 6, 28–36.
- Miller, C. (1982) *Philos. Trans. R. Soc. London B* 299, 401–411.
- Miller, C., & Richard, E. A. (1990) in *Chloride Channels and Carriers in Nerve, Muscle, and Glial Cells* (Alvarez-Leefmans, F. J., & Russell, J. M., Eds.) pp 383–405, Plenum Publishing Corporation, New York.
- O'Neill, G. P., Grygorczyk, R., Adam, M., & Ford-Hutchinson, A. W. (1991) *Biochim. Biophys. Acta* 1129, 131–134.
- Palade, P. T., & Barchi, R. L. (1977) *J. Gen. Physiol.* 69, 879–896.
- Parcej, D. N., & Dolly, J. O. (1989) *Biochem. J.* 257, 899–903.
- Park, C.-S., Hausdorff, S. F., & Miller, C. (1991) *Proc. Natl. Acad. Sci. U.S.A.* 88, 2046–2050.
- Popot, J.-L., & Changeux, J.-P. (1984) *Physiol. Rev.* 64, 1162–1239.
- Ran, S., & Benos, D. J. (1992) *J. Biol. Chem.* 267, 3618–3625.
- Redhead, C. R., Edelman, A. E., Brown, D., Landry, D. W., & Al-Awqati, Q. (1992) *Proc. Natl. Acad. Sci. U.S.A.* 89, 3716–3720.
- Rettig, J., Heinemann, S. H., Wunder, F., Lorra, C., Parcej, D. N., Dolly, J. O., & Pongs, O. (1994) *Nature* 369, 289–294.
- Reynolds, J. A., & Karlin, A. (1978) *Biochemistry* 17, 1035–2038.
- Rosenthal, E. R., & Guidotti, G. (1994) *Biochim. Biophys. Acta* 1191, 256–266.
- Schaffner, W., & Weissmann, C. (1973) *Anal. Biochem.* 56, 502–514.
- Sigworth, F. J. (1994) *Q. Rev. Biophys.* 27, 1–40.
- Slinde, E., & Flatmark, T. (1976) *Biochim. Biophys. Acta* 455, 796–805.
- Sobel, A., Weber, M., & Changeux, J.-P. (1977) *Eur. J. Biochem.* 80, 215–224.
- Steinmeyer, K., Ortland, C., & Jentsch, T. J. (1991) *Nature* 354, 301–304.
- Steinmeyer, K., Lorenz, C., Pusch, M., Koch, C., & Jentsch, T. J. (1994) *EMBO J.* 13, 737–743.
- Thiemann, A., Gründer, S., Pusch, M., & Jentsch, T. J. (1992) *Nature* 356, 57–60.
- Uchida, S., Sasaki, S., Furukawa, T., Hiraoka, M., Imai, T., Hirata, Y., & Maruma, F. (1993) *J. Biol. Chem.* 268, 3821–3824.
- Unwin, N. (1993) *J. Mol. Biol.* 229, 1101–1124.
- White, M. M., & Miller, C. (1981) *J. Gen. Physiol.* 78, 1–18.
- Woodbury, D. J., & Miller, C. (1990) *Biophys. J.* 58, 833–839.
- Yellen, G., Jurman, M., Abramson, T., & MacKinnon, R. (1991) *Science* 251, 939–942.